Liposomal delivery of a Pin1 inhibitor complexed with cyclodextrins as new therapy for high-grade serous ovarian cancer

Concetta Russo Spena[1,2], Lucia De Stefano[1,2], Stefano Palazzolo[1], Barbara Salis[3,4], Carlotta Granchi[5], Filippo Minutolo[5], Tiziano Tuccinardi[5], Roberto Fratamico[6], Sara Crotti[7], Sara D'Aronco[7], Marco Agostini[7,8], Giuseppe Corona[9], Isabella Caligiuri[4], Vincenzo Canzonieri[4] and Flavio Rizzolio[1,10]

1. Experimental and Clinical Pharmacology, Department of Translational Research, National Cancer Institute and Center for Molecular Biomedicine - CRO, Aviano, Italy.

2. Doctoral School in Chemistry, University of Trieste, Italy.

3. Doctoral School in Molecular Biomedicine, University of Trieste, Italy.

4. Pathology Unit, Department of Molecular Biology and Translational Research, National Cancer Institute and Center for Molecular Biomedicine - CRO, Aviano, Italy.

5. Department of Pharmacy, University of Pisa, Italy.

6. Department of Medical Oncology, Sidney Kimmel Cancer Center, Thomas Jefferson University, Philadelphia, PA.

7. Institute of Pediatric Research-Città della Speranza, Padova, Italy.

8. First Surgical Clinic Section, Department of Surgical, Oncological and Gastroenterological Sciences, University of Padova, Italy.

9. Immunopathology and Cancer Biomarkers Unit, Department of Molecular Biology and Translational Research, National Cancer Institute and Center for Molecular Biomedicine - CRO, Aviano, Italy.

10. Department of Molecular Sciences and Nanosystems, Ca' Foscari University, Venezia-Mestre, Italy.

Keywords: Pin1, ovarian cancer, liposome, inhibitory small molecules.

ABSTRACT

Pin1, a prolyl isomerase that sustains tumor progression, is overexpressed in different types of malignancies. Functional inactivation of Pin1 restrains tumor growth and leaves normal cells unaffected making it an ideal pharmaceutical target. Although many studies on Pin1 have focused on malignancies that are influenced by sex hormones, studies in ovarian cancer have lagged behind. Here, we show that Pin1 is an important therapeutic target in high-grade serous epithelial ovarian cancer. Knock down of Pin1 in ovarian cancer cell lines induces apoptosis and restrains tumor growth in a syngeneic mouse model. Since specific and non-covalent Pin1 inhibitors are still limited, the first liposomal formulation of a Pin1 inhibitor was designed. The drug was efficiently encapsulated in modified cyclodextrins and remotely loaded into pegylated liposomes. This liposomal formulation accumulates preferentially in the tumor and has a desirable pharmacokinetic profile. The liposomal inhibitor was able to alter Pin1 cancer driving-pathways trough the induction of proteasome-dependent degradation of Pin1 and was found to be effective in curbing ovarian tumor growth *in vivo*.

INTRODUCTION

High-grade serous epithelial ovarian cancer (HGSOC) is a deadly disease, which accounts for more than 150.000 deaths each year worldwide [1]. For decades, treatment strategies for HGSOC have shown little improvement in overall survival and the use of cytoreductive surgery followed by platinum-based chemotherapy remains the first-line treatment [1–3]. Although most patients respond to platinum based therapy, the majority relapse and die from the disease [4–9]. Lack of knowledge regarding tumor origin has been the major limitation in the discovery of new therapeutic agents. Only recently, new mouse models have clarified that secretory epithelial cells of the distal fallopian tube (FTSECs) are the likely progenitors of a substantial proportion of HGSOCs [10–14]. In addition, progress in the molecular characterization of tumors derived directly from patients have defined important pathways for the development and progression of HGSOCs [15,16]. Alterations of homologous recombination, PI3K/RAS, RB, NOTCH, and FOXM1 pathways are commonly found [15].

A fundamental mechanism in controlling key proteins in these pathways is the phosphorylation of the proline (Pro)-Ser/Thr motifs, which are controlled by the Peptidyl-prolyl *cis-trans* isomerase NIMA-interacting 1 (Pin1), a unique Peptidyl-prolyl isomerase (PPIase) [17,18]. Pin1 accelerates the conversion of *cis* and *trans* isomers, which is slowed down by phosphorylation. The net result is the activation of oncogenes and inactivation of tumor suppressor genes in cancer cells [19–27]; therefore, its inhibition represents an exciting therapeutic target for the treatment of HGSOCs. In addition, Pin1 possesses other unique features which are attractive as a therapeutic target: a) the PPIase domain has a specific, structurally-organized shaped active site that is suitable for drug development [28]; b) mice knocked down (KD) for Pin1 are viable without gross abnormalities [29] and c) genetic manipulation of Pin1 in several oncogene-induced mouse models of tumorigenesis limits tumor burden and metastatic spread [30]. Pin1 is

63 expressed at low levels in normal tissues and specifically upregulated in cancer cells and cancer
64 stem cells, a subclass of neoplastic cells found in most tumors which are more resistant to
65 commonly used chemotherapy drugs [31]. Furthermore, inhibition of Pin1 sensitizes cancer cells
66 to targeted- and chemo-therapies and reverses drug resistance [32,33]. Many research groups and
67 companies are developing Pin1 ligands; however, in spite of highly specific molecular inhibition,
68 they lack demonstrated effective inhibition of Pin1 and antitumor activity *in vivo* [34]. In turn, no
69 clinical trials have been performed due to inadequate pharmacological parameters of developed
70 inhibitors such as potency, solubility, and cell permeability [35]. Only recently, it has been
71 discovered a specific Pin1 inhibitor possessing an *in vivo* activity, albeit with a covalent
72 mechanism of action [36].

73 A current approach in improving pharmacokinetic (PK) parameters and toxicity profile of drugs
74 is the development of nanoparticles for drug delivery [37]. Nanodrugs have many fundamental
75 properties that are necessary in cancer therapy: specific accumulation in the tumor taking
76 advantage of enhanced permeability and retention (EPR) effect [38], increased therapeutic ratio
77 (high effectiveness and low toxicity) and improved drug solubility. Although thousands of
78 nanomaterials are under investigation, liposomes, a bilayer of lipids that mimic the cell
79 membrane are of great interest [39–41]. Other than biocompatibility, these nanomaterials have
80 already been approved by the Food and Drug Administration in the United States and the
81 European Medicines Agency in Europe [42–45].

82 Here we demonstrated that Pin1 is overexpressed in ovarian cancer tissue samples and when
83 knocked down, promotes ovarian cancer cell death *in vitro* and *in vivo* demonstrating its
84 potential as pharmacological cancer target for HGSOC. For the first time, we encapsulated a
85 selective Pin1 inhibitor (compound 17 in Guo *et al*.,) designed by Pfizer into liposomes. This
86 small molecule is among the most potent Pin1 inhibitors but with low solubility and poor

permeability [34]. Utilizing a similar method developed by Vogelstein's group [46], we successfully loaded the drug/modified cyclodextrin complex by remote loading into liposomes and utilized it to kill ovarian cancer cells in an *in vivo* model.

2. Experimental section

2.1 Materials

Liposomal formulation

1,2-distearoyl-*sn*-glycero-3-phosphocholine (DSPC), cholesterol, 1,2- dipalmitoyl-*sn*-glycero-3-phosphoethanolamine-N-[methoxy(polyethylene glycol)-2000] (DPPE-PEG), polycarbonate membranes from Avanti Polar Lipids (Alabaster, AL, US). Heptakis-(6-amino-6-deoxy)-β-Cyclodextrin 7xHCl, CDexB-013 from Arachem (Netherlands). Slide-A-Lyzer® MINI Dialysis Devices, 20K MWCO from ThermoFisher Scientific (Waltham, MA, US). Instrumentation: DLS Zetasizer Nano ZSP (ZEN 5600) from Malvern Instruments (United Kingdom). NanoDrop 2000c from ThermoFisher Scientific (Waltham, MA, US).

In vitro experiments

Tissue microarrays: OV2001 and OV802 from US Biomax Inc. (Rockville, MD, US). Antibody rabbit PIN1 1:50 (sc-15340) from Santa Cruz (Santa Cruz, CA, US). Instrumentation: Benchmark ultra instrument from Ventana Medical Systems (Tucson, AZ, US).

Cell cultures: OVCAR3, MRC-5, T47D, PLC/PRF/5 and NIH-3T3 cell lines from ATCC (Manassas, VA, US). Kuramochi and COV318 cell lines were generously provided by Gustavo Baldassarre. STOSE cell line was generously provided by Barbara Vanderhyden.

shRNA: Human Pin1 KD1 (TRCN0000001033), KD2 (TRCN0000010577) and mouse Pin1 KD1 (TRCN0000012580), KD2 (TRCN0000012582) from Sigma-Aldrich Merck (Germany).

Oligonucleotides: m/h Pin1-f: 5-CAAGGAGGAGGCCCTGGAGC; m/h Pin1-r: 5-TGCA TCTGACCTCTGCTGAAGG; m HPRT-f: 5-AGTACTTCAGGGATTTGAATCACG; m

HPRT-r: 5- GGACTCCTCGTATTTGCAGATTC; βact-Fw: 5- GACCCAGATCATGTTTGAGA; βact-rev: GACTCCATGCCCAGGAAG from IDT Technology (Coralville, IA, US).

Flow cytometry analysis: propidium iodide and RNase A from Roche (Switzerland). PE-Annexin V Apoptosis Detection Kit from Becton-Dickinson (Franklin Lakes, NJ, US). Instrumentation and software: for sub G1 analysis, FACscan instrument from Becton-Dickinson (Franklin Lakes, NJ, US) and ModFit LTV4.0.5 (Win) software; for Annexin V analysis, FACS Canto II from Becton-Dickinson (Franklin Lakes, NJ, US) and BD FACS DIVA software.

Cell viability and caspase 3/7 assays: CellTiter-Glo®luminescent cell viability assay and caspase 3/7 Glo assay from Promega (Madison, WI, US). NP-40 lysis buffer: 0.01 M Tris-HCl, 0.01 M NaCl, 0.003 M $MgCl_2$, 0.03 M sucrose, and 0.5% NP-40. Instrumentation: F200 Tecan instrument from Tecan (Switzerland). The IC_{50} was calculated using the GraphPad program from Prism (La Jolla, CA, US).

RNA analysis: Smarter Nucleic Acid Sample Preparation kit from Stratec biomedical (Germany). Go-Script RT System kit and GoTaq® G2 Polymerase and Master Mix from Promega (Madison, WI, US).

Western blot analysis: phosphatase inhibitors (Complete-EDTA free) from Roche (Switzerland). TruePage Precast Gels 4-12 % SDS-PAGE from Sigma-Aldrich Merck (Germany). Amersham TM Protran TM 0.45 µm NC from GE Healthcare Life Science (Pittsburgh, PA, US). RIPA buffer: 10 mM Tris-Cl (pH 8.0), 1% NP-40, 0.1% sodium deoxycholate, 0.1% SDS, 140 mM NaCl. Antibodies: mouse Cyclin D1 1:1000 (556470) from BD Pharmigen™ (Franklin Lakes, NJ, US); rabbit β-catenin 1:1000 (#8480S), rabbit β-actin 1:1000 (#4967S) and rabbit HA-tag (#3724S) from Cell Signaling Technology (Danvers, MA, US); rabbit LC3B 1:1000

(GTX127375) from GeneTex (Irvine, CA, US); rabbit Pin1 1:250 (sc-15340), mouse Pin1 1:250 (sc-46660) and mouse Hsp70 1:1000 (sc-24) from Santa Cruz (Santa Cruz, CA, US); rabbit α-tubulin 1:2000 (T9026) from Sigma-Aldrich Merck (Germany). Secondary antibodies anti-rabbit (31464, 1:5000) and anti-mouse (31432, 1:5000) from ThermoFisher Scientific (Waltham, MA, US). Software: Image J (NIH).

In vivo experiments

Liquid chromatography tandem mass spectrometry (LC-MS/MS): Ultra-grade acetonitrile and formic acid (>98 %) from Romil LTD (United Kingdom). Instrumentation: Qiagen Tissue Ruptor from Qiagen (Germantown, MD, US). UltiMate 3000 system from ThermoFisher Scientific, (Waltham, MA, US) coupled to an API 4000 triple quadrupole mass spectrometer from AB SCIEX (Framingham, MA, US) working in multiple reaction monitoring (MRM) modality. Hypersil GOLD C8 column 2.1 × 100 mm, 3 µm, from ThermoFisher Scientific (Waltham, MA, US). Milli-Q Academic/Quantum EX system from Millipore (Milford, MA, US).

Biodistribution, PK and Tumor growth: 8 week-old female FVB/N mice and 6 week-old female athymic nude FOXN1^{NU} mice from Envigo (United Kingdom). Cultrex® Basement Membrane Matriz, Type 3 from Trevigen (Gaithersburg, MD, US).

2.2 Methods

2.2.1 *Liposomal formulation*

A representative Pin1 inhibitor (compound 8, Scheme S1; compound 17 in Guo *et al*.,[34]), belonging to the alkyl amide indole-based library of compounds developed by Pfizer was synthesized in our laboratory following the previously reported procedure [34] (see Supplemental methods).

157 Pegylated liposomes: DSPC, cholesterol and DPPE-PEG (50:45:5, molar ratio) were dissolved in
158 chloroform (20 mL). The solvent was removed by vacuum to form a thin lipid film, which was
159 hydrated by shaking in the appropriate buffer (80 mM Arg·Hepes, pH 9) at 65 °C for 2 h. The
160 vesicle suspension was serially extruded through 0.4-, 0.2- and 0.1- μm polycarbonate
161 membranes, 10 times for each membrane, at 65 °C to obtain mono-dispersed liposomes. The
162 transmembrane gradient was then created by dialyzing liposomes overnight in PBS. The average
163 size and polydispersity index were measured by dynamic light scattering experiments.
164 Cyclodextrin-Inhibitor (CI) complex: compound 8 was dissolved in methanol and mixed with
165 equimolar quantity of Heptakis-(6-amino-6-deoxy)-β-Cyclodextrin 7xHCl in deionized water. In
166 detail, the methanolic solution of the drug was added in a dropwise fashion to the cyclodextrin
167 solution in agitation (final concentration of methanol was 10%). This suspension was shaken at
168 55 °C for 48 h. The solution was flash-frozen in a dry ice/acetone bath followed by
169 lyophilization and then stored at −20 °C until further use.

170 Liposomes/cyclodextrin/compound 8 (LC8) complex: After lyophilization, CI was incubated
171 with 20 mg/mL of liposomal solution for 1 h at 65 °C. The sample was spun at 13.8xg for 5 sec
172 in order to remove the particulate matter. The amount of compound 8 loaded within the
173 liposomes was determined by UV-VIS method utilizing a calibration curve. The compound 8 and
174 LC8 were dissolved in methanol and analyzed at 270 nm.

175 The loading efficiency of compound 8 was evaluated after disruption of the liposomal solution
176 with methanol: 5 μl of LC8 was dissolved in 600 μl of methanol. The rate of release of
177 compound 8 from the liposomes was evaluated using a dialysis membrane at 37° C in PBS 1X. It
178 was utilized 1mg/ml of compound 8 in the LC8 formulation.

179 2.2.2 *In vitro experiments*

Immunohistochemical analysis

Human ovarian carcinoma and normal ovarian tissue microarrays were incubated with Pin1 antibody for 1 h at room temperature utilizing the ultraview DAB detection kit with CC1 buffer for 36 min in Benchmark ultra instrument.

The ovarian tissues were analyzed with light microscopy using 10 and 20X magnifications. The immunohistochemical (IHC) staining was converted to an H score: intensity (0, 1, 2, 3) x area (0-100%). The H score from 0 to 75 (first quartile) was defined as low expression and > 75 was defined as medium-high expression. Two pathologists scored IHC staining independently.

All mouse tissues were fixed for 24 h in formalin and embedded in paraffin. Each slide was 3 μm thick, counterstained with hematoxylin/eosin and analyzed at 20/40X of magnification. IHC of Pin1 was done using the same criteria as human tissues.

Flow cytometry, caspase 3/7 and cell viability analyses

OVCAR3, MRC-5, T47D, PLC/PRF/5 and NIH3T3 cell line grown as indicated by supplier. Kuramochi and COV318 cell line grown in RPMI and DMEM media with 10% FBS, respectively. STOSE cell line grown in DMEM media with 4% FBS. Pin1 knock down experiments were performed as previously described [23]. Briefly polyclonal populations of transduced cells were generated by infection with 1 MOI (multiplicity of infectious units) of shRNA lentiviral particles.

Sub G1 analysis: cells were fixed by adding ice-cold 70% ethanol while vortexing. Fixed cells were stored at 4 °C for at least 2 h and then washed once with PBS. Cells were stained with 1 μg/ml propidium iodide, 500 ng/ml RNase A in PBS and incubated at room temperature for 1 h in the dark. Sub G1 analysis was performed after 5 days.

Annexin V analysis was performed according to the manufacturer's protocol. Cells were stained with PE Annexin V and 7-AAD and incubated for 30 min at room temperature in the dark. 300 µl of 1X binding buffer were added to each tube. Samples were evaluated within 1 h. Annexin V analysis was performed after 5 days.

Caspase 3/7 assay: $1x10^5$ cells were lysed in 10 µl of NP-40 buffer and incubated with 10 µl of caspase 3/7 kit for 1 h at room temperature. Caspase 3/7 assay was done after 3 days.

Cell viability: the cells were infected with three different plasmids: two knock down and a control. Three days after infection the cells were seeded in 96-well plates at a density of 10^3 cells/well. The viability was evaluated by luminescent assay. Averages and standard deviations were obtained from triplicates.

RT-PCR, Real-time PCR and western blot analyses

Reverse transcription: 400 ng of total RNA were prepared from cells using the Smarter Nucleic Acid Preparation kit and were reverse transcribed in a 10 µl reaction using Go-Script RT System kit. 4 ng of cDNA were used to amplify target genes.

Semi-quantitative PCR: cDNA was amplified using GoTaq® G2 Polymerase and Master Mix. Hprt was used as a control. PCR reactions were carried out in a final volume of 20 µL as described in the manufacturer's protocol. The PCR cycles were as follow: 5 min at 95 °C; 20 s at 95 °C, 30 s at 60 °C, 30 s at 72 °C x 30 cycles. The products were analyzed via 3% agarose gel electrophoresis.

Western blot analysis: Total cell extracts were obtained by treating cells with RIPA buffer 0.1% SDS plus protease and phosphatase inhibitors then incubate on ice for 20 min and sonicated for 5

s. After centrifuging at 13.8xg for 20 min at 4 °C, equal amount of protein (50 µg) was separated by TruePage Precast Gels. Proteins were transferred onto nitrocellulose membranes, then blocked for 30 min with 5% non-fat dried milk in TBS containing 0.1% Tween 20 (TBS-T). The membranes were incubated with primary antibodies at 4 °C ON, washed three times with TBS-T and incubated with HRP-conjugated secondary antibodies for 1 h at room temperature. The results were visualized by ECL western blot analysis detection system.

Half maximal inhibitory concentration (IC_{50})

In order to evaluate the IC_{50} of compound 8 and LC8, cells were plated in a 96-well plate one day before treatment (OVCAR3: 10^3 cells/well; MRC-5: 10^4 cells/well). Then the cells were treated with LC8, cyclodextrin/compound 8, liposome/compound 8, compound 8 or empty liposomes starting with a concentration of 100 µM followed by five 1:2 serial dilutions. After 96 h, the cell viability and IC_{50} was evaluated by luminescent assay.

Pin1 stability

$3x10^5$ NIH3T3 cells were plated one day before treatment. Cells were treated with 0, 50 and 100 µM of LC8, collected after 48 h and analyzed by RT-PCR or cells were treated with 100 µM of LC8 and DMSO as control for 24 h followed by 10 µg/mL of cycloheximide (CHX). Cells were collected after 0, 3, 6, 12 and 24 h for western blot analysis. Cells were also treated with 0, 50 and 100 µM of LC8 for 48 h and then treated with MG132 10 µM and after 6 h collected for western blot analysis.

Pin1 target analysis

T47D, PLC/PRF/5 and OVCAR3 were seeded with a density of $5x10^5$ in 100 x 20 mm tissue culture dish one day before treatment. The cells were treated with 100 µM of compound 8 (LC8)

and with 10 μM ATRA for 24 h and collected for western blot analysis.

2.2.3 *In vivo experiments*

Animal studies

Animal studies were done in accordance to the Italian Governing Law (D.lgs 26/2014) under the authorization of Ministry of Health n° 788/2015-PR and performed in accordance with the institutional guidelines. Data are reported as the mean and standard error.

Immunocompetent tumor model: 10^7/1ml STOSE cells were injected i.p. into 8 week-old female FVB/N mice.

Immunodeficient tumor model: $5x10^6$ OVCAR3 cell line were mixed 1:1 with DMEM w/o phenol red/ Cultrex-Type 3 and implanted subcutaneously into the flank of 6 week-old female athymic nude FOXN1^{NU} mice. When tumors reached the size of 168±28 mm^3, mice were treated i.p. with LC8 one time per week for three treatments. Tumor volumes were measured with a caliper and calculated using the formula: (length×$width^2$)/ 2.

PK: the experiment was performed in 8 weeks-old FVB/N mice treated with 20 mg/kg (i.p.) of LC8 diluted in PBS 1X. 100 μl of blood were collected after 10 min, 3, 6, 12 and 24 h and analyzed by LC-MS/MS. A total of 200 μl were drawn from each mouse.

Biodistribution: female nude mice were treated at a dose of 20 mg/kg of compound 8 (LC8) and sacrificed after 72 h. The organs were washed by perfusion with 10 ml of cold PBS/heparin before collection, diluted in 500 μl of PBS/BSA 4%, and homogenized with Qiagen Tissue Ruptor for 20 s at power 4 on ice. Samples were stored at -80 °C. The concentrations of inhibitor were measured by LC-MS/MS.

LC-MS/MS

Before extraction, a known amount of internal standard (IS) solution (Guo *et al*.,[34], compound 16) was added to PK and biodistribution samples. Then, acetonitrile/0.1 % formic acid was added (final volume ratio, 1:2). The samples were vortexed and placed into a sonicator bath for 5 min at 4 °C. This procedure was repeated twice and after centrifugation (13.8xg, 20 min, 4 °C), supernatants were collected together and dried under vacuum (Univapo 150 H). Calculated extraction recoveries are reported in Table S1. Five-point calibration curves within the analyte concentration ranges 0.6–2857.1 ng/ml and 0.2–95 ng/ml were prepared in blank serum and tissue samples, obtained from untreated mice.

Selected transitions for Compound 8 and IS were as follows: m/z 423.1 > 206.1 and m/z 423.1 > 218.1 for Compound 8; m/z 391.1 > 206.2 and m/z 391.1 > 188.1 for IS. The optimized ESI (+) source parameters are reported in Table S1. Chromatographic separation was performed on a Hypersil GOLD C8 column. Elution was achieved by a linear gradient (mobile phase A: 0.1 % formic acid, mobile phase B: acetonitrile/0.1 % formic acid) from 30 % to 95 % B over 4 min. Injection volume was 10 µl and flow rate was 300 µl/min.

2.3 Statistical analysis

The statistical significance was determined using the two-tails paired t-test, unless specified. A p-value less than 0.05 was considered significant for all comparisons done.

3. Results and discussion

3.1 Pin1 expression is altered in serous ovarian cancer patients

Pin1 controls many oncogenes and tumor suppressor genes and for this reason is of wide interest as a therapeutic target. Prior studies have focused on malignancies including breast and prostate cancer [47,48], however this is the first that deeply investigates Pin1 in ovarian cancer. As a first step, we took advantage of the whole genome data released from The Cancer Genome Atlas (TCGA) consortium. The data were filtered for the presence of multiple alterations (amplification, deletion and mutation) in different tumor types. Fig. S1 showed that Pin1 is mostly altered in hormonal cancers with HGSOC in the top position.

In support of the genomic amplification of Pin1, it has been reported to be frequently increased at the protein level in different types of cancers [49–54] and it is a good prognostic factor in hormone-dependent tumors [20,48]. A few analyses focused specifically on ovarian cancer [55]. To strength these data, we have analyzed by IHC 167 cases of serous ovarian cancer on tissue microarray (TMA). Among these, 59.4% were grade 3. The expression values were divided into two categories: low and medium-high (see Experimental section). In Fig. 1A, an example of these categories was reported. When compared to adjacent normal tissue (13 cases), Pin1 is significantly upregulated (p-value 0.0012, Fisher exact test) (Fig. 1B). Taking our data and the results from the TCGA into consideration, we concluded that Pin1 deserved further investigation as potential therapeutic target in ovarian cancer.

A

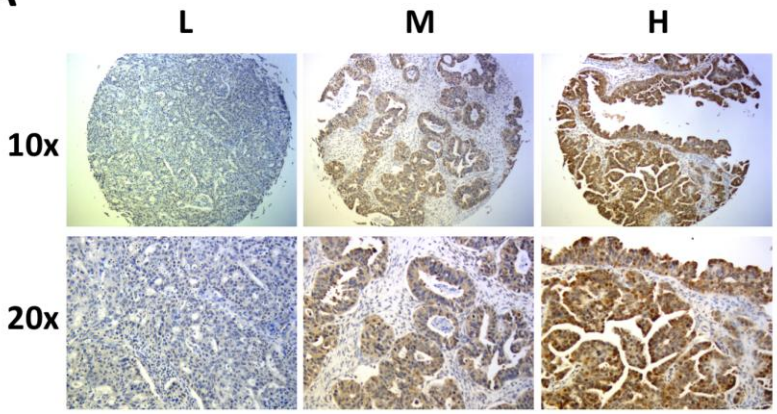

B

	Pin1		
	Low	Mid-High	Total
Serous	**77** (42.8%)	**90** (50%)	**167** (92.8%)
Normal	**12** (6.7%)	**1** (0.5%)	**13** (7.2%)
Total	**89** (49.4%)	**91** (50.6%)	**180** (100%)
p_value	**0.0012**		

Fig. 1. *Pin1 is highly expressed in HGSOC. (A) Representative images of Pin1 categorized as low (L), medium (M) and high (H) expression at different magnifications. (B) Pin1 protein is upregulated in cancer vs normal tissues. Fifty percent of cancer tissues have medium-high expression of Pin1 compared to 0.5% in normal tissues.*

3.2 Pin1 knock-down reduces tumor cell growth in vitro and shRNA treated cells implanted in vivo in a syngeneic model of HGSOC

To understand if Pin1 is a valid therapeutic target in HGSOC, we knocked down its expression in different ovarian cancer cell lines that recently have been demonstrated to closely represent ovarian cancer patients [56–58]. Firstly, Pin1 activity was evaluated in a spontaneously transformed mouse ovarian surface epithelial cancer cell line (STOSE), which strictly recapitulates the characteristics of human HGSOC [59]. Fig. 2A shows that mouse shRNAs efficiently down regulate the expression of Pin1. Pin1 knock down (KD) cells were less viable

than normal cells and its upregulation increases cell viability (two side t-test, p-value < 0.05), (Fig. 2B). Since STOSE cell lines derived from FVB/N mice (syngeneic), normal and knock down cells were injected intraperitoneally (i.p.). Fig. 2C demonstrates that Pin1 KD abolishes tumor formation after >3 months of follow up.

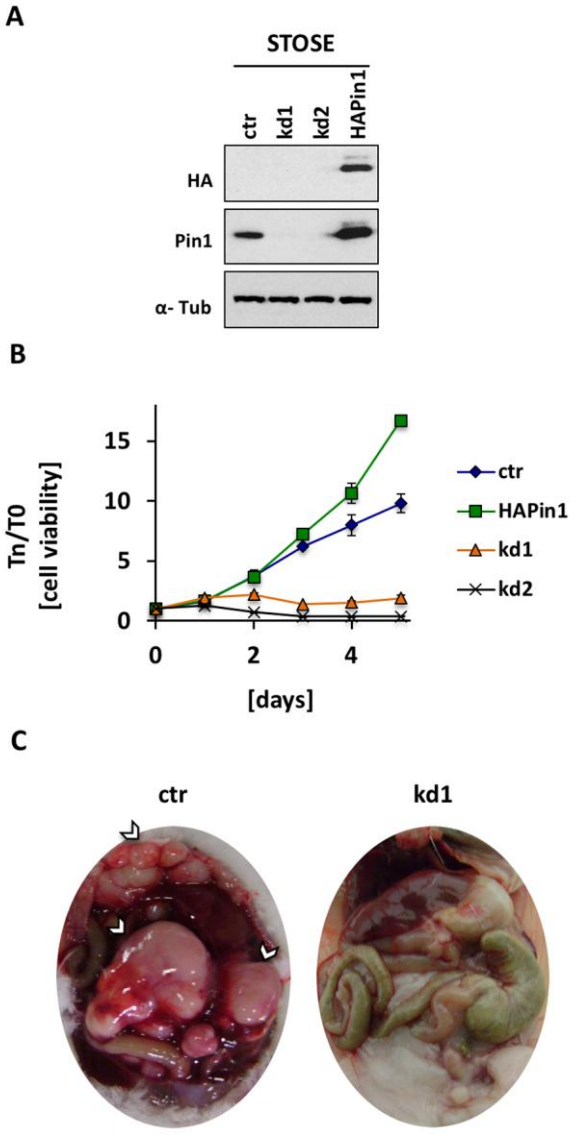

Fig. 2*. Pin1 knock-down reduces tumor cell growth in vitro and shRNA treated cells implanted in vivo in a syngeneic model of HGSOC. (A) Western blot analysis of Pin1 downregulation (kd) and upregulation (HaPin1) in STOSE cells. (B) Cell viability of STOSE cells (Pin1 wild type, kd and overexpress) were monitored for 5 days. Values on y-axis: ratio between luminescence values at day n*

(Tn) normalized to day 0 (T0). (C) Representative images of FVB/N mice injected i.p. with STOSE cells wild type or kd for Pin1 (n=3).

3.3 Pin1 knock down induces cell death in human HGSOC cell lines

In order to evaluate if Pin1 affects cell viability in human cells, Kuramochi, COV318, and OVCAR3 cell lines were KD (Fig. 3A) and followed for 6 days. Pin1 KD cells were less viable than control cells (Fig. 3B).

The population of sub-G1 cells was evaluated in the same human cell lines, which showed an increase in sub-G1 phase in Pin1 KD cells (two side t-test, p-value < 0.05), (Fig. 3C). To discriminate if a real apoptotic mechanism was activated, cells were analysed for Annexin V staining. The knock down cells have an increased number of apoptotic cells (early and total apoptosis) compared to normal cells (two side t-test, p-value < 0.05), (Fig. 3D,E). To gain insight into the molecular mechanism that leads to apoptosis, caspase 3/7 were evaluated. The activity of these protease enzymes is increased in knock down cells (two side t-test, p-value < 0.05) (Fig. 3F).

In conclusion, the results obtained from human and mouse HGSOC models confirmed that Pin1 is a valid therapeutic target for HGSOC patients.

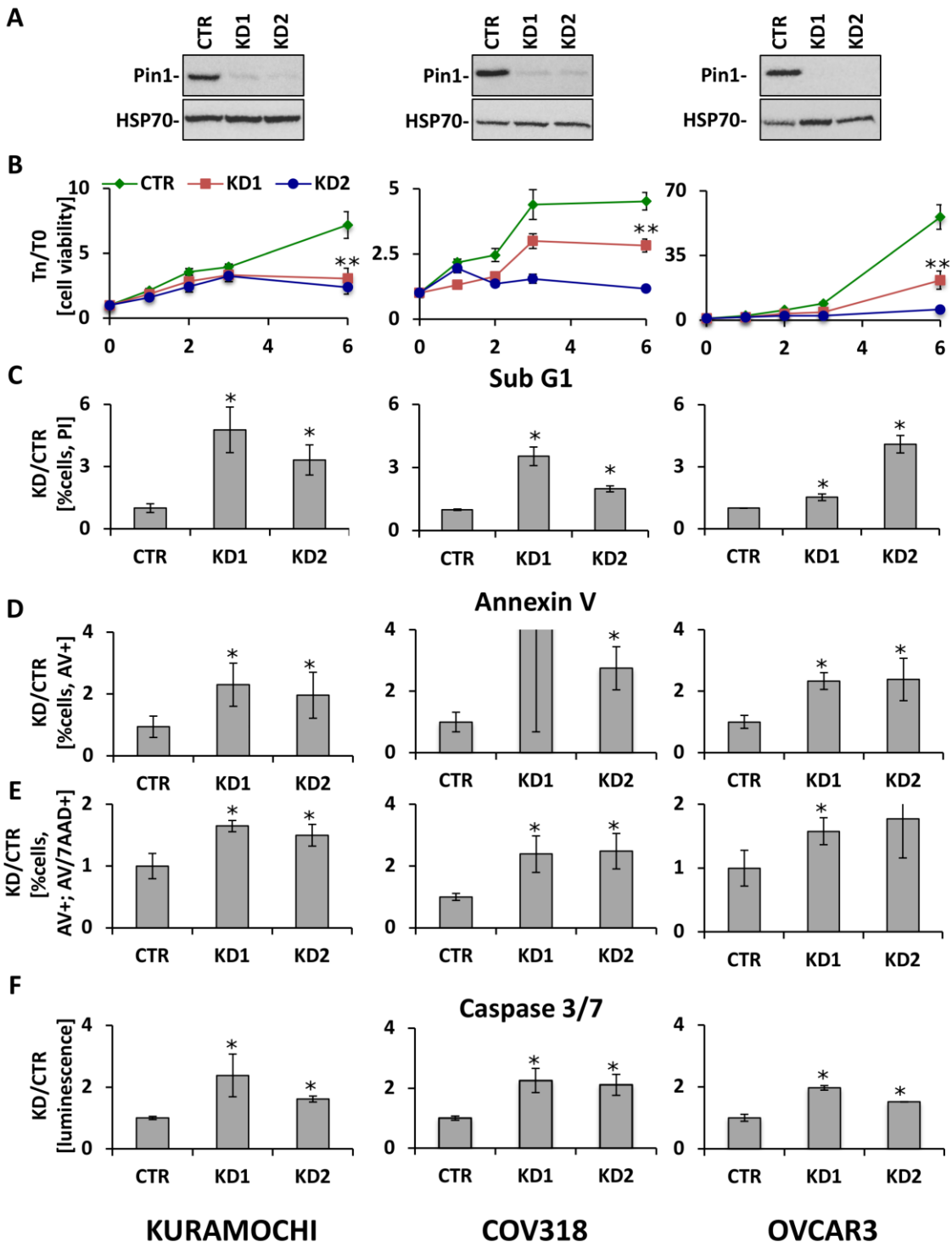

Fig. 3. Pin1 knock down induces apoptosis in ovarian cancer cell lines. Pin1 was KD in Kuramochi, COV318, and Ovcar3 cell lines. (A) Western blot analysis demonstrates the KD efficiency. (B) Cell viability was done in triplicates. X axis: days. (C) Sub G1 was determined by propidium iodide staining (≥ three independent experiments). (D) Early and (E) total apoptosis were determined by Annexin V/7-

AAD staining (≥ three independent experiments). (F) Activation of caspase 3/7 was analyzed on cell extracts by luminescence assay (≥ two independent experiments). All the values on y-axis are normalized to the control. (, p value < 0.05).*

3.4 Liposomal/cyclodextrin/compound 8 (LC8) has desired pharmacological properties

Liposomal nanoparticles have been successful utilized as treatments for different diseases [60]. The major advantages are biocompatibility and an improved therapeutic window [61]. Unfortunately, only weakly acidic or basic drugs could be stably incorporated inside the cores of liposomes [62]. Recently, the Vogelstein group demonstrated that a hydrophobic drug could be solubilized in physiologic buffers and remote loaded into liposomes by modified cyclodextrins that have the properties of weak bases or acids [46].

A representative Pin1 inhibitor (compound 8, scheme S1), belonging to the alkyl amide indole-based library of compounds developed by Pfizer, was synthesized in our laboratory since it was among the most potent inhibitors of the isolated enzyme, showing a *Ki* value of 75 nM. This compound could be easily synthesized but it has a low solubility in water and is ineffective in cancer cells [34,63,64]. Compound 8 was solubilized in Heptakis (6-amino-6-deoxy)-ß-cyclodextrins and loaded into pegylated-liposomes (see Experimental section for details). Compound 8 has a solubility of 0.30±0.05 mg/ml. When formulated as a liposomal/cyclodextrin complex (Fig. 4A), the solubility of the Pin1 inhibitor increased by about 6 times (1.82±0.10 mg/ml) (Fig. 4B). The loading efficiency of LC8 evaluated by UV absorbance was of 91.2±5.0 percent (expressed as loaded /total drug ratio) (Fig. 4C). The hydrodynamic size of liposomes under different temperatures was determined by DLS. The size increased from 25 to 37 °C and remained stable up to 65 °C (Fig. S2A). The measures pre and post loading showed a low polydispersity index with the size of liposomes that increase from 151.8±0.10 nm (pre) to

177±0.11 nm (post) (Fig. 4D). The ability of LC8 to retain compound 8 was then tested. Fig. 4E demonstrates that the release from a semipermeable membrane of LC8 was slower than inhibitor alone. The accumulation of compound 8 into the liposome and the slow release rate may contribute to the change in the *in vivo* pharmacological properties. As proof of concept, LC8 was tested on OVCAR3 cells. Although compound 8 has no activity, LC8 has an IC_{50} value in the low micromolar range (Fig. 4F and Fig. S2B). LC8 has no activity on MRC-5 normal fibroblasts (data not shown). These results allowed us to test LC8 in an *in vivo* mouse model.

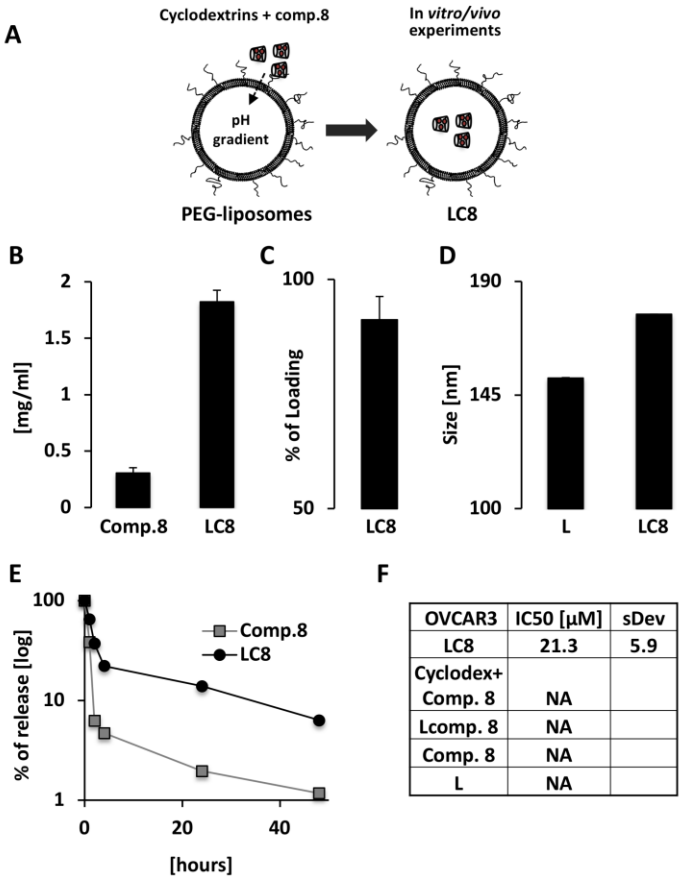

OVCAR3	IC50 [µM]	sDev
LC8	21.3	5.9
Cyclodex+ Comp. 8	NA	
Lcomp. 8	NA	
Comp. 8	NA	
L	NA	

Fig. 4. *LC8: chemico-physical properties and in vitro activity. (A) Schematic representation of the active loading of compound 8 (Comp.8) into pegylated liposomes. (B) LC8 increases the solubility of comp. 8 in PBS solution by about 6 times. (C) The loading efficiency of comp. 8 into pegylated liposomes is more than 90%. (D) DLS analysis of liposomes before (L) and after loading of LC8. (E) Release of comp. 8 or LC8 through a semipermeable membrane. Representative result. (F) OVCAR3 cell line was treated with*

LC8, cyclodextrin/comp. 8, liposome/comp. 8, comp. 8, or empty liposomes (L) and the IC50 was determined after 96 hours (NA: Not applicable).

3.5 LC8 promotes Pin1 protein degradation

High affinity or covalent inhibitors promote degradation of Pin1 [36,65]. To assess the effect of LC8, fibroblast cells were treated with 100 µM of LC8. We observed that LC8 caused a decrease in the level of the Pin1 protein (Fig. 5A). At the mRNA level, the treatment did not substantially alter Pin1 (Fig. 5B). To discriminate between protein degradation or decreased stability, cells were treated with MG132 (proteasome inhibitor) (Fig. 5A) or CHX (protein synthesis inhibitor) (Fig. 5C). Only MG132 rescued the expression of Pin1 confirming a specific mechanism of protein degradation mediated by the proteasome.

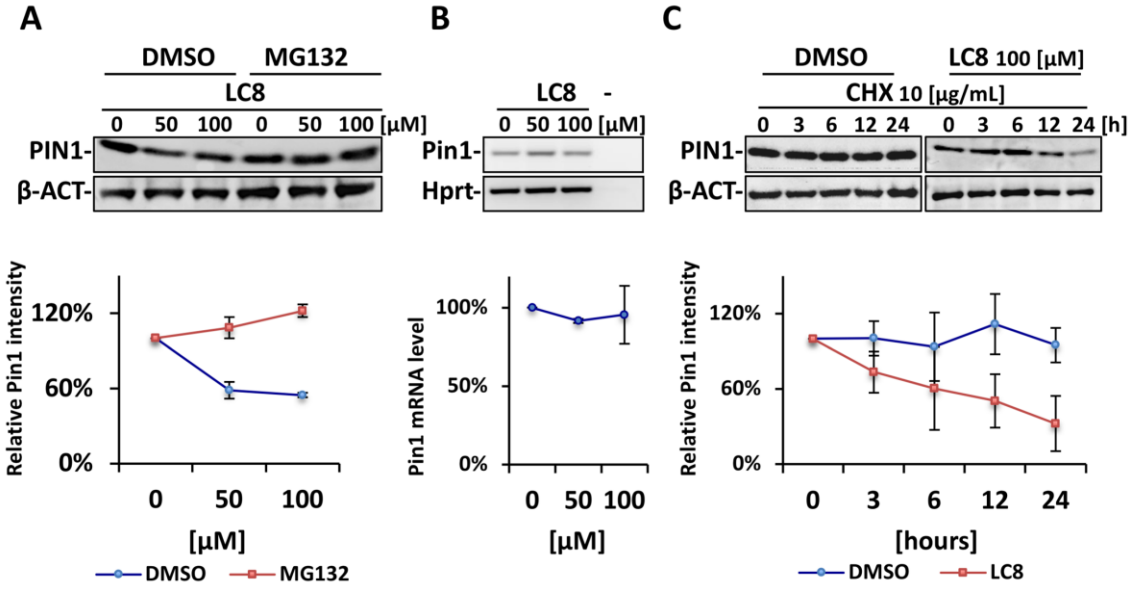

Fig. 5. *LC8 induces Pin1 degradation through the proteasome. (A) Fibroblasts were treated with 100 µM of LC8 for 48 hours followed by 10 µM of proteasomal inhibitor MG132 for 6 hours. MG132 was able to rescue the expression of Pin1 protein. (B) Fibroblasts were treated as in (A). Pin1 RNA levels was unaffected. (C) Fibroblasts were treated with 100 µM of LC8 for 24 hours followed by 10 µg/ml of CHX*

for the indicated time. LC8 induces protein degradation through the proteasome. Bottom panel: semiquantitative analysis was reported.

3.6 LC8 alters the levels and function of PIN1 substrates

Pin1 controls multiple cancer drive-pathways through regulation of many oncogenes and tumor suppressor genes at various levels [27]. We utilized T47D (breast) and PLC/PRF/5 (liver) cancer cell lines as published models and OVCAR3 cell line to study LC8's effect [36,66]. Compared to untreated cells, LC8 downregulated the expression of ß-catenin, LC3B (autophagy), and cyclin D1 (cell cycle; only in OVCAR3 cells) (Fig. 6). As control we utilized ATRA, a recently published inhibitor of Pin1 [65], which provided similar results.

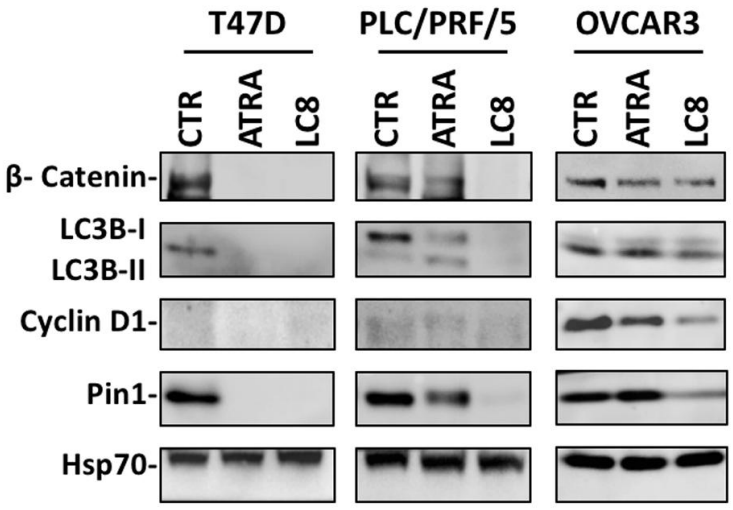

Fig. 6. *LC8 alters the expression of Pin1 target proteins. T47D, PLC/PRF/5 and OVCAR3 cell lines were treated with 10 μM of ATRA (positive control) and 100 μM of LC8 for 24 hours and analyzed by western blot. The expression of β-catenin, LC3B, and cyclin D1 was down regulated by LC8.*

3.7 LC8 is a drug for HGSOC therapy

Liposomal drugs are mostly effective *in vivo* due to their designed formulation to accumulate inside the tumor (EPR effect) and increase drug solubility. Before testing the efficacy of LC8, we carried out a maximum tolerated dose (MTD) experiments. Mice were treated with a dose

418 escalation of the liposomal formulation (without drug) and the health of the mice was monitored
419 (body weight and histopathology analysis). We found that the mice could be treated up to 250
420 mg/kg without evident signs of toxicity (Fig. S3A,B). Afterwards, the mice were treated i.p. with
421 LC8 at the indicated doses. As an objective scale of mouse health, the body weight was followed
422 for almost 3 months. We observed no sign of toxicity up to 40 mg/kg (Fig. S4A,B).

423 OVCAR3 cells are a good model of HGSOC and can grow subcutaneously in nude mice. Cells
424 were injected into the flank of the mice and after tumors reached a volume of 168±28 mm^3, the
425 animals were treated with 20 mg/kg of LC8 as in the MTD experiment. LC8 significantly
426 decreased tumor volume compared to untreated mice (Fig. 7A). The body weight of the mice in
427 both groups remained unchanged (Fig. 7B). Serum PK analysis of the drug showed two-kinetic
428 phases of elimination, with a major decrement in the first 10 h (Fig. 7C). Interestingly, the
429 biodistribution of LC8 after 72 h showed a main accumulation in the tumor followed by liver,
430 spleen, and skin (Fig. 7D). Similar to Doxil[41], the liposomal formulation could avoid
431 accumulation of doxorubicin in tissues with tight junctions and a well-developed lymphatic
432 system such as in the heart. On the contrary, tumors with leaky vasculature and a poor lymphatic
433 system allowed the accumulation of LC8, in turn increasing the efficacy of the drug. Although
434 the circulation time of LC8 is far from Doxil, the volume of distribution is still low thus
435 increasing the therapeutic index.

436 The effect of LC8 was evaluated on the expression of Pin1 in the tumors of mice treated with
437 LC8 or untreated (PBS) as in Fig. 7A and B. LC8 downregulated the expression of Pin1 at
438 background level (negative) as showed in Fig. 7E. In untreated mice, Pin1 has an intense
439 cytoplasmic/nuclear staining.

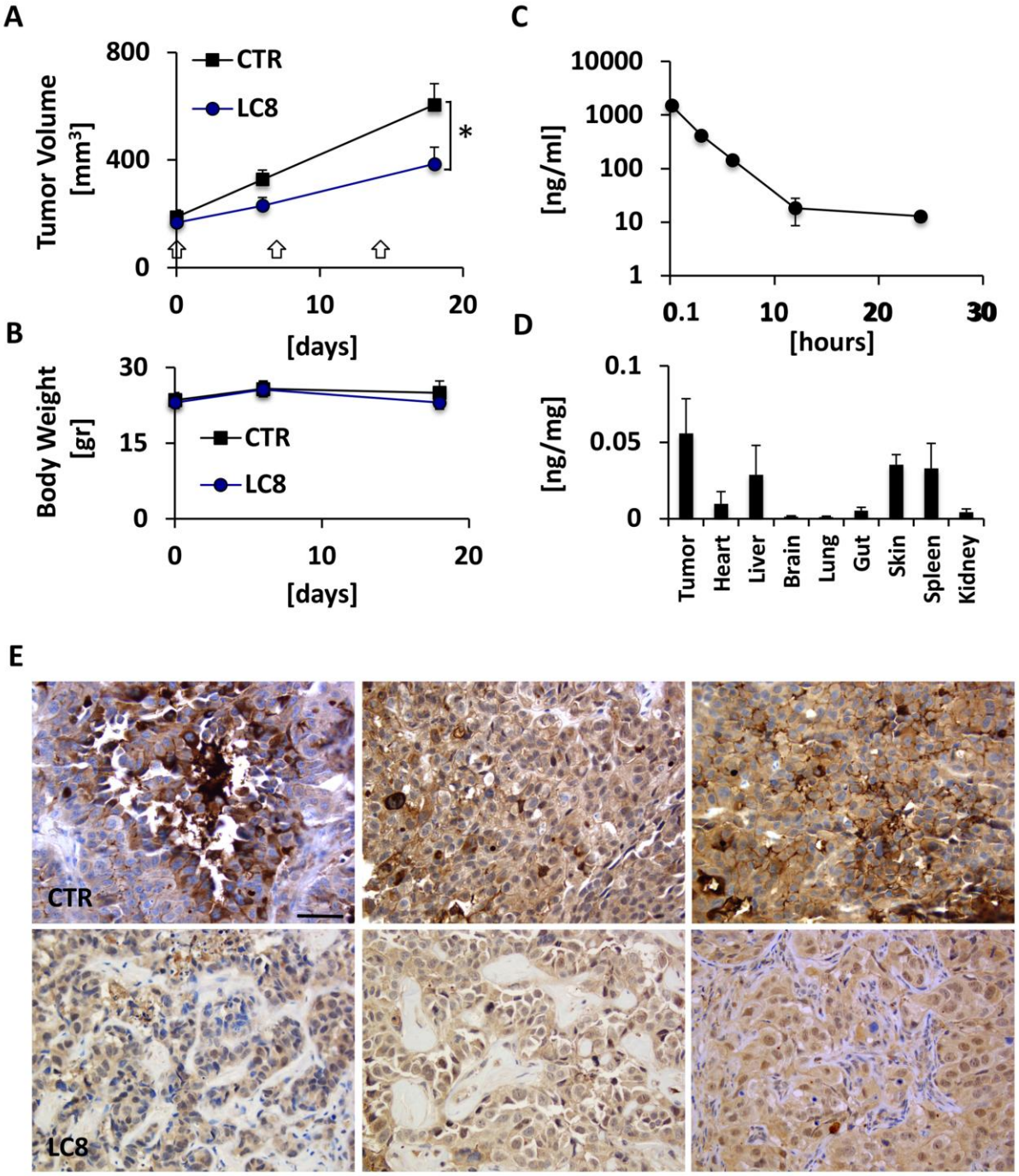

440

441 ***Fig. 7.*** *LC8 is effective in a HGSOC mouse tumor model. Nude mice were subcutaneously injected with*
442 *5x10^6 OVCAR3 cell line (n=12, group) and (A) tumor volume and (B) body weight were followed for 18*
443 *days. LC8 was injected i.p. every 7 days (arrows) at a dose of 20 mg/kg. LC8 was effective to reduce*
444 *tumor burden without compromising animal health. (C) FVB/N mice (n=3, data point) were i.p. injected*
445 *with 20 mg/kg of LC8 and plasma was analyzed at indicated time point. Y axis: ng of drug/ml of blood*

(D) Nude mice (n=3, data point) subcutaneously implanted with OVCAR3 cell line were i.p. injected with 20 mg/kg of LC8 and analyzed after 72 hours. Y axis: ng of drug/mg of tissue. LC8 accumulated mainly in the tumor. (E) IHC evaluation of Pin1 expression in 3 tumors derived from (A and B). Scale bar: 100 μm.

4. Conclusions

This investigation is the first to report the preparation of an effective liposomal formulation of a potent and selective Pin1 inhibitor. The new nanoformulation improves the *in vitro* and in *vivo* pharmacological properties of the Pin1 inhibitor. We showed that Pin1 is overexpressed in human serous ovarian cancer and its inhibition induces cell death and tumor growth reduction in mouse metastatic immunocompetent ovarian and human subcutaneous ovarian cancer models. The development of such new active liposome formulations may pave the way for clinical experimentation and support for a new effective targeted therapy for ovarian cancer patients.

5. Funding Sources

My First AIRC (No. 1569)

6. Acknowledgments

Authors are grateful and would like to recognize the Associazione Italiana per la Ricerca sul Cancro –AIRC. Mrs. Laura Zannier and Antonella Selva for histopathology experiments.

Competing interests

The authors declare no competing interests.

References

[1] D.D. Bowtell, S. Böhm, A.A. Ahmed, P.-J. Aspuria, R.C. Bast, V. Beral, et al., Rethinking ovarian cancer II: reducing mortality from high-grade serous ovarian cancer., Nat. Rev. Cancer. 15 (2015) 668–79.

[2] G.C. Jayson, E.C. Kohn, H.C. Kitchener, J.A. Ledermann, Ovarian cancer, Lancet. 384 (2014) 1376–1388. doi:10.1016/S0140-6736(13)62146-7.

[3] C. Della Pepa, G. Tonini, C. Pisano, M. Di Napoli, S.C. Cecere, R. Tambaro, et al., Ovarian cancer standard of care: are there real alternatives?, Chin. J. Cancer. 34 (2015) 17–27. doi:10.5732/cjc.014.10274.

[4] B. Kaufman, R. Shapira-Frommer, R.K. Schmutzler, M.W. Audeh, M. Friedlander, J. Balmaña, et al., Olaparib Monotherapy in Patients With Advanced Cancer and a Germline *BRCA1/2* Mutation, J. Clin. Oncol. 33 (2015) 244–250. doi:10.1200/JCO.2014.56.2728.

[5] P.C. Fong, D.S. Boss, T.A. Yap, A. Tutt, P. Wu, M. Mergui-Roelvink, et al., Inhibition of Poly(ADP-Ribose) Polymerase in Tumors from *BRCA* Mutation Carriers, N. Engl. J. Med. 361 (2009) 123–134. doi:10.1056/NEJMoa0900212.

[6] E. Pujade-Lauraine, F. Hilpert, B. Weber, A. Reuss, A. Poveda, G. Kristensen, et al., Bevacizumab Combined With Chemotherapy for Platinum-Resistant Recurrent Ovarian Cancer: The AURELIA Open-Label Randomized Phase III Trial, J. Clin. Oncol. 32 (2014) 1302–1308. doi:10.1200/JCO.2013.51.4489.

[7] C. Aghajanian, S. V Blank, B.A. Goff, P.L. Judson, M.G. Teneriello, A. Husain, et al., OCEANS: a randomized, double-blind, placebo-controlled phase III trial of chemotherapy with or without bevacizumab in patients with platinum-sensitive recurrent epithelial

ovarian, primary peritoneal, or fallopian tube cancer., J. Clin. Oncol. 30 (2012) 2039–45. doi:10.1200/JCO.2012.42.0505.

[8] T.J. Perren, A.M. Swart, J. Pfisterer, J.A. Ledermann, E. Pujade-Lauraine, G. Kristensen, et al., A Phase 3 Trial of Bevacizumab in Ovarian Cancer, N. Engl. J. Med. 365 (2011) 2484–2496. doi:10.1056/NEJMoa1103799.

[9] R.A. Burger, M.F. Brady, M.A. Bookman, G.F. Fleming, B.J. Monk, H. Huang, et al., Incorporation of Bevacizumab in the Primary Treatment of Ovarian Cancer, N. Engl. J. Med. 365 (2011) 2473–2483. doi:10.1056/NEJMoa1104390.

[10] R. Perets, G.A. Wyant, K.W. Muto, J.G. Bijron, B.B. Poole, K.T. Chin, et al., Transformation of the fallopian tube secretory epithelium leads to high-grade serous ovarian cancer in Brca;Tp53;Pten models., Cancer Cell. 24 (2013) 751–65. doi:10.1016/j.ccr.2013.10.013.

[11] A. Flesken-Nikitin, C.-I. Hwang, C.-Y. Cheng, T. V. Michurina, G. Enikolopov, A.Y. Nikitin, Ovarian surface epithelium at the junction area contains a cancer-prone stem cell niche, Nature. 495 (2013) 241–245. doi:10.1038/nature11979.

[12] S. Vaughan, J.I. Coward, R.C. Bast, A. Berchuck, J.S. Berek, J.D. Brenton, et al., Rethinking ovarian cancer: recommendations for improving outcomes., Nat. Rev. Cancer. 11 (2011) 719–25. doi:10.1038/nrc3144.

[13] J. Kim, D.M. Coffey, C.J. Creighton, Z. Yu, S.M. Hawkins, M.M. Matzuk, High-grade serous ovarian cancer arises from fallopian tube in a mouse model, Proc. Natl. Acad. Sci. 109 (2012) 3921–3926. doi:10.1073/pnas.1117135109.

[14] C.A. Sherman-Baust, E. Kuhn, B.L. Valle, I.-M. Shih, R.J. Kurman, T.-L. Wang, et al., A

genetically engineered ovarian cancer mouse model based on fallopian tube transformation mimics human high-grade serous carcinoma development, J. Pathol. 233 (2014) 228–237. doi:10.1002/path.4353.

[15] Integrated genomic analyses of ovarian carcinoma., Nature. 474 (2011) 609–15. doi:10.1038/nature10166.

[16] H. Zhang, T. Liu, Z. Zhang, S.H. Payne, B. Zhang, J.E. McDermott, et al., Integrated Proteogenomic Characterization of Human High-Grade Serous Ovarian Cancer, Cell. 166 (2016) 755–765. doi:10.1016/j.cell.2016.05.069.

[17] M.B. Yaffe, M. Schutkowski, M. Shen, X.Z. Zhou, P.T. Stukenberg, J.U. Rahfeld, et al., Sequence-specific and phosphorylation-dependent proline isomerization: a potential mitotic regulatory mechanism., Science. 278 (1997) 1957–60.

[18] R. Ranganathan, K.P. Lu, T. Hunter, J.P. Noel, Structural and functional analysis of the mitotic rotamase Pin1 suggests substrate recognition is phosphorylation dependent., Cell. 89 (1997) 875–86.

[19] M. Gianni, A. Boldetti, V. Guarnaccia, A. Rambaldi, E. Parrella, I. Raska Jr., et al., Inhibition of the peptidyl-prolyl-isomerase Pin1 enhances the responses of acute myeloid leukemia cells to retinoic acid via stabilization of RARalpha and PML-RARalpha, Cancer Res. 69 (2009) 1016–1026. doi:0008-5472.CAN-08-2603 [pii]10.1158/0008-5472.CAN-08-2603.

[20] J.E. Girardini, M. Napoli, S. Piazza, A. Rustighi, C. Marotta, E. Radaelli, et al., A Pin1/mutant p53 axis promotes aggressiveness in breast cancer, Cancer Cell. 20 (2011) 79–91. doi:S1535-6108(11)00226-1 [pii]10.1016/j.ccr.2011.06.004.

[21] P. Zacchi, M. Gostissa, T. Uchida, C. Salvagno, F. Avolio, S. Volinia, et al., The prolyl isomerase Pin1 reveals a mechanism to control p53 functions after genotoxic insults., Nature. 419 (2002) 853–7. doi:10.1038/nature01120.

[22] R. La Montagna, I. Caligiuri, P. Maranta, C. Lucchetti, L. Esposito, M.G. Paggi, et al., Androgen receptor serine 81 mediates Pin1 interaction and activity., Cell Cycle. 11 (2012) 3415–20.

[23] F. Rizzolio, C. Lucchetti, I. Caligiuri, I. Marchesi, M. Caputo, A.J. Klein-Szanto, et al., Retinoblastoma tumor-suppressor protein phosphorylation and inactivation depend on direct interaction with Pin1, Cell Death Differ. 19 (2012) 1152–61. doi:cdd2011202 [pii]10.1038/cdd.2011.202.

[24] C. Lucchetti, I. Caligiuri, G. Toffoli, A. Giordano, F. Rizzolio, The Prolyl Isomerase Pin1 Acts Synergistically with CDK2 to Regulate the Basal Activity of Estrogen Receptor α in Breast Cancer., PLoS One. 8 (2013) e55355. doi:10.1371/journal.pone.0055355.

[25] R. La Montagna, I. Caligiuri, A. Giordano, F. Rizzolio, Pin1 and nuclear receptors: A new language?, J. Cell. Physiol. 228 (2013) 1799–801. doi:10.1002/jcp.24316.

[26] F. Rizzolio, I. Caligiuri, C. Lucchetti, R. Fratamico, V. Tomei, G. Gallo, et al., Dissecting Pin1 and phospho-pRb regulation, J Cell Physiol. 228 (2013) 73–7. doi:10.1002/jcp.24107.

[27] X.Z. Zhou, K.P. Lu, The isomerase PIN1 controls numerous cancer-driving pathways and is a unique drug target, Nat. Rev. Cancer. 16 (2016) 463–478. doi:10.1038/nrc.2016.49.

[28] J.D. Moore, A. Potter, Pin1 inhibitors: Pitfalls, progress and cellular pharmacology, Bioorg. Med. Chem. Lett. 23 (2013) 4283–4291. doi:10.1016/j.bmcl.2013.05.088.

[29] Y.C. Liou, A. Ryo, H.K. Huang, P.J. Lu, R. Bronson, F. Fujimori, et al., Loss of Pin1

556 function in the mouse causes phenotypes resembling cyclin D1-null phenotypes, Proc Natl
557 Acad Sci U S A. 99 (2002) 1335–1340. doi:10.1073/pnas.032404099032404099 [pii].

558 [30] Z. Lu, T. Hunter, Prolyl isomerase Pin1 in cancer, Cell Res. 24 (2014) 1033–1049.
559 doi:10.1038/cr.2014.109.

560 [31] A. Singh, J. Settleman, EMT, cancer stem cells and drug resistance: an emerging axis of
561 evil in the war on cancer, Oncogene. 29 (2010) 4741–4751. doi:10.1038/onc.2010.215.

562 [32] A. Rustighi, A. Zannini, L. Tiberi, R. Sommaggio, S. Piazza, G. Sorrentino, et al., Prolyl-
563 isomerase Pin1 controls normal and cancer stem cells of the breast., EMBO Mol. Med. 6
564 (2014) 99–119. doi:10.1002/emmm.201302909.

565 [33] Q. Ding, L. Huo, J.-Y. Yang, W. Xia, Y. Wei, Y. Liao, et al., Down-regulation of Myeloid
566 Cell Leukemia-1 through Inhibiting Erk/Pin 1 Pathway by Sorafenib Facilitates
567 Chemosensitization in Breast Cancer, Cancer Res. 68 (2008) 6109–6117.
568 doi:10.1158/0008-5472.CAN-08-0579.

569 [34] C. Guo, X. Hou, L. Dong, J. Marakovits, S. Greasley, E. Dagostino, et al., Structure-based
570 design of novel human Pin1 inhibitors (III): Optimizing affinity beyond the phosphate
571 recognition pocket, Bioorg. Med. Chem. Lett. 24 (2014) 4187–4191.
572 doi:10.1016/j.bmcl.2014.07.044.

573 [35] I.P. A J Sinclair G Peters, and P J Farrell, EBNA-2 and EBNA-LP cooperate to cause G0
574 to G1 transition during immortalization of resting human B lymphocytes by Epstein-Barr
575 virus., EMBO J. 13 (1994).

576 [36] E. Campaner, A. Rustighi, A. Zannini, A. Cristiani, S. Piazza, Y. Ciani, et al., A covalent
577 PIN1 inhibitor selectively targets cancer cells by a dual mechanism of action, Nat.

578 Commun. 8 (2017) 15772. doi:10.1038/ncomms15772.

579 [37] E. Blanco, H. Shen, M. Ferrari, Principles of nanoparticle design for overcoming
580 biological barriers to drug delivery, Nat. Biotechnol. 33 (2015) 941–951.
581 doi:10.1038/nbt.3330.

582 [38] Y. Matsumura, H. Maeda, A new concept for macromolecular therapeutics in cancer
583 chemotherapy: mechanism of tumoritropic accumulation of proteins and the antitumor
584 agent smancs., Cancer Res. 46 (1986) 6387–92.

585 [39] K. Greish, Enhanced Permeability and Retention (EPR) Effect for Anticancer
586 Nanomedicine Drug Targeting, in: Methods Mol. Biol., 2010: pp. 25–37.
587 doi:10.1007/978-1-60761-609-2_3.

588 [40] S. Palazzolo, S. Bayda, M. Hadla, I. Caligiuri, G. Corona, G. Toffoli, et al., The Clinical
589 translation of Organic Nanomaterials for Cancer Therapy: A Focus on Polymeric
590 Nanoparticles, Micelles, Liposomes and Exosomes, Curr. Med. Chem. 24 (2017).
591 doi:10.2174/0929867324666170830113755.

592 [41] S. Bayda, M. Hadla, G. Corona, G. Toffoli, F. Rizzolio, F. Rizzolio, Inorganic
593 Nanoparticles for Cancer Therapy: a Transition from Lab to Clinic, Curr. Med. Chem. 25
594 (2017). doi:10.2174/0929867325666171229141156.

595 [42] Y. Barenholz, Doxil®--the first FDA-approved nano-drug: lessons learned., J. Control.
596 Release. 160 (2012) 117–34. doi:10.1016/j.jconrel.2012.03.020.

597 [43] E. Miele, G.P. Spinelli, E. Miele, F. Tomao, S. Tomao, Albumin-bound formulation of
598 paclitaxel (Abraxane ABI-007) in the treatment of breast cancer., Int. J. Nanomedicine. 4
599 (2009) 99–105.

[44] U. Bulbake, S. Doppalapudi, N. Kommineni, W. Khan, Liposomal Formulations in Clinical Use: An Updated Review, Pharmaceutics. 9 (2017) 12. doi:10.3390/pharmaceutics9020012.

[45] D. Bobo, K.J. Robinson, J. Islam, K.J. Thurecht, S.R. Corrie, Nanoparticle-Based Medicines: A Review of FDA-Approved Materials and Clinical Trials to Date, Pharm. Res. 33 (2016) 2373–2387. doi:10.1007/s11095-016-1958-5.

[46] S. Sur, A.C. Fries, K.W. Kinzler, S. Zhou, B. Vogelstein, Remote loading of preencapsulated drugs into stealth liposomes, Proc. Natl. Acad. Sci. 111 (2014) 2283–2288. doi:10.1073/pnas.1324135111.

[47] M. Napoli, J.E. Girardini, S. Piazza, G. Del Sal, Wiring the oncogenic circuitry: Pin1 unleashes mutant p53, Oncotarget. 2 (2011) 654–656. doi:329 [pii].

[48] G. Ayala, D. Wang, G. Wulf, A. Frolov, R. Li, J. Sowadski, et al., The prolyl isomerase Pin1 is a novel prognostic marker in human prostate cancer, Cancer Res. 63 (2003) 6244–6251.

[49] P.B. Lam, L.N. Burga, B.P. Wu, E.W. Hofstatter, K.P. Lu, G.M. Wulf, Prolyl isomerase Pin1 is highly expressed in Her2-positive breast cancer and regulates erbB2 protein stability., Mol. Cancer. 7 (2008) 91. doi:10.1186/1476-4598-7-91.

[50] K.-W. Leung, C.-H. Tsai, M. Hsiao, C.-J. Tseng, L.-P. Ger, K.-H. Lee, et al., Pin1 overexpression is associated with poor differentiation and survival in oral squamous cell carcinoma., Oncol. Rep. 21 (2009) 1097–104.

[51] P. Jawanjal, S. Salhan, I. Dhawan, R. Tripathi, G. Rath, Peptidyl-prolyl isomerase Pin1-mediated abrogation of APC-β-catenin interaction in squamous cell carcinoma of cervix.,

622 Rom. J. Morphol. Embryol. 55 (2014) 83–90.

623 [52] C.-X. Zhou, Y. Gao, Aberrant expression of beta-catenin, Pin1 and cylin D1 in salivary
624 adenoid cystic carcinoma: relation to tumor proliferation and metastasis., Oncol. Rep. 16
625 (2006) 505–11.

626 [53] F.-C. Lin, Y.-C. Lee, Y.-G. Goan, C.-H. Tsai, Y.-C. Yao, H.-C. Cheng, et al., Pin1
627 positively affects tumorigenesis of esophageal squamous cell carcinoma and correlates
628 with poor survival of patients., J. Biomed. Sci. 21 (2014) 75. doi:10.1186/s12929-014-
629 0075-1.

630 [54] J. Kuramochi, T. Arai, S. Ikeda, J. Kumagai, H. Uetake, K. Sugihara, High Pin1
631 expression is associated with tumor progression in colorectal cancer, J. Surg. Oncol. 94
632 (2006) 155–160. doi:10.1002/jso.20510.

633 [55] L. Bao, A. Kimzey, G. Sauter, J.M. Sowadski, K.P. Lu, D.G. Wang, Prevalent
634 overexpression of prolyl isomerase Pin1 in human cancers, Am J Pathol. 164 (2004)
635 1727–1737.

636 [56] S. Domcke, R. Sinha, D.A. Levine, C. Sander, N. Schultz, Evaluating cell lines as tumour
637 models by comparison of genomic profiles., Nat. Commun. 4 (2013) 2126.
638 doi:10.1038/ncomms3126.

639 [57] K.L. Thu, M. Papari-Zareei, V. Stastny, K. Song, M. Peyton, V.D. Martinez, et al., A
640 comprehensively characterized cell line panel highly representative of clinical ovarian
641 high-grade serous carcinomas., Oncotarget. 8 (2017) 50489–50499.
642 doi:10.18632/oncotarget.9929.

643 [58] A.K. Mitra, D.A. Davis, S. Tomar, L. Roy, H. Gurler, J. Xie, et al., In vivo tumor growth

644 of high-grade serous ovarian cancer cell lines, Gynecol. Oncol. 138 (2015) 372–377.
645 doi:10.1016/j.ygyno.2015.05.040.

646 [59] C.W. McCloskey, R.L. Goldberg, L.E. Carter, L.F. Gamwell, E.M. Al-Hujaily, O. Collins,
647 et al., A new spontaneously transformed syngeneic model of high-grade serous ovarian
648 cancer with a tumor-initiating cell population., Front. Oncol. 4 (2014) 53.
649 doi:10.3389/fonc.2014.00053.

650 [60] H.-I. Chang, M.-K. Yeh, Clinical development of liposome-based drugs: formulation,
651 characterization, and therapeutic efficacy., Int. J. Nanomedicine. 7 (2012) 49–60.
652 doi:10.2147/IJN.S26766.

653 [61] A. Gabizon, H. Shmeeda, Y. Barenholz, Pharmacokinetics of pegylated liposomal
654 Doxorubicin: review of animal and human studies., Clin. Pharmacokinet. 42 (2003) 419–
655 36. doi:10.2165/00003088-200342050-00002.

656 [62] J. Gubernator, Active methods of drug loading into liposomes: recent strategies for stable
657 drug entrapment and increased *in vivo* activity, Expert Opin. Drug Deliv. 8 (2011) 565–
658 580. doi:10.1517/17425247.2011.566552.

659 [63] L. Dong, J. Marakovits, X. Hou, C. Guo, S. Greasley, E. Dagostino, et al., Structure-based
660 design of novel human Pin1 inhibitors (II)., Bioorg. Med. Chem. Lett. 20 (2010) 2210–4.
661 doi:10.1016/j.bmcl.2010.02.033.

662 [64] C. Guo, X. Hou, L. Dong, E. Dagostino, S. Greasley, R. Ferre, et al., Structure-based
663 design of novel human Pin1 inhibitors (I)., Bioorg. Med. Chem. Lett. 19 (2009) 5613–6.
664 doi:10.1016/j.bmcl.2009.08.034.

665 [65] S. Wei, S. Kozono, L. Kats, M. Nechama, W. Li, J. Guarnerio, et al., Active Pin1 is a key

target of all-trans retinoic acid in acute promyelocytic leukemia and breast cancer, Nat. Med. 21 (2015) 457–466. doi:10.1038/nm.3839.

[66] X.-H. Liao, A.L. Zhang, M. Zheng, M.-Q. Li, C.P. Chen, H. Xu, et al., Chemical or genetic Pin1 inhibition exerts potent anticancer activity against hepatocellular carcinoma by blocking multiple cancer-driving pathways, Sci. Rep. 7 (2017) 43639. doi:10.1038/srep43639.